Dominant source regions of the Earth's "hum" are coastal

Peter D. Bromirski[1] and Peter Gerstoft[1]

Received 27 April 2009; revised 1 June 2009; accepted 10 June 2009; published 3 July 2009.

[1] Hum beam power observations using the USArray EarthScope transportable array, combined with infragravity wave observations, show that the dominant source area of the Earth's hum over the 120–400 s period band during winter months is the Pacific coast of North America, with the western coast of Europe a secondary source region. Correlation of hum with model ocean wave heights indicates that the Pacific coast of Central America is an important hum source region when impacted by austral storm waves. Hum is excited by relatively local infragravity wave forcing as ocean swell propagates along coasts, with no indication of significant deep-ocean hum generation. **Citation:** Bromirski, P. D., and P. Gerstoft (2009), Dominant source regions of the Earth's ''hum'' are coastal, *Geophys. Res. Lett.*, *36*, L13303, doi:10.1029/2009GL038903.

1. Introduction

[2] The continuous vibration of the Earth's normal modes, commonly referred to as Earth's ''hum'' [*Nishida et al.*, 2000], are excited at nearly constant levels in the absence of large earthquakes [*Suda et al.*, 1998]. The source of the Earth's hum has been linked to excitation by infragravity waves [*Rhie and Romanowicz*, 2004; *Tanimoto*, 2005; *Webb*, 2007, 2008; *Uchiyama and McWilliams*, 2008], with direct coupling of atmospheric forcing [*Suda et al.*, 1998; *Nishida and Kobayashi*, 1999; *Nishida et al.*, 2000] now considered not a significant factor [*Webb*, 2008]. Infragravity (IG) waves are generated along coasts by the non-linear transformation of incident swell into longer period IG wave energy [*Herbers et al.*, 1995a, 1995b]. As IG wave amplitudes depend on swell amplitudes impacting coasts, there is a clear connection between storm track and intensity on the dominant location of hum excitation and hum levels, both seasonally and longer term. Recent studies suggest that hum is excited by infragravity waves in the deep ocean [*Rhie and Romanowicz*, 2004; *Webb*, 2008] and also over shallow continental shelves [*Webb*, 2007, 2008]. Modeling suggests that deep-ocean IG wave energy can provide sufficient forcing to account for hum background levels [*Tanimoto*, 2005; *Webb*, 2008; *Uchiyama and McWilliams*, 2008]. However, sufficiently long duration, large-scale, broadband ocean-bottom observations at hum frequencies have not been made to determine whether hum is excited by IG waves in the deep ocean or primarily over continental shelves. Because IG wave amplitudes are much higher over the shelf than the deep ocean [*Webb et al.*, 1991] and because of the frequency-dependent exponential decay of wave pressure with depth, it seems more likely that continental shelves are the dominant hum source area.

2. Approach

[3] The dominant hum source areas were identified using back azimuth estimates from continuous beamformed vertical-component data at 292 stations of the USArray EarthScope transportable array (TA). These TA stations have an aperture of 2000 × 1200 km (3 × 1.8 λ at 6mHz), sufficiently large to resolve hum source region back azimuths using hum Rayleigh waves.

[4] The array data were beamformed as described by *Gerstoft and Tanimoto* [2007]. To reduce earthquake noise, amplitudes that exceeded 0.5 standard deviations of the one-hour quietest daily values were set to that threshold. 4096-s data segments (1 Hz sampling) was Fourier transformed, with only the phase retained and combined into one complex-valued vector $\mathbf{v}(\omega, t_i)$ from the signal phases at each station in the array, where t_i refers to the start time of the Fourier transform. The plane-wave response for the seismic array is given by $\mathbf{p}(\omega, \psi, s) = \exp(i\,\omega\,\mathbf{re}\,s)$, where s is slowness, $\mathbf{r}$ describes the coordinates of the array relative to the mean coordinates, and $\mathbf{e}$ contains the direction cosines of the plane wave for a given azimuth ψ. The beamformer output is given by $\mathbf{b}(\omega, t, \psi, s) = |\mathbf{p}(\omega, \psi, s)^T \mathbf{v}(\omega, t)|^2$. Thus, the maximum beam power for any combination of [azimuth, slowness] is $\mathbf{v}(\omega, t)^T\mathbf{v}(\omega, t)$. The array 3-dB beamwidth is 0.15 s/km for a vertically incident 0.006 Hz plane wave. 25 FFT frequency bins were stacked across the 400–120 s period band, and along the Rayleigh wave phase slowness from 0.22–0.26 s/km (4.5–3.8 km/s phase velocity). This gives the best-fitting plane wave over azimuth during each segment, and allows determination of hum source area on synoptic time scales.

3. West Coast of North America Hum Generation

[5] Beam power across the TA from November 2006 to June 2007 (Figure 1a) shows concentrations at particular azimuths, associated with the seasonal cycle, i.e. the shift in storms from Northern to Southern Hemisphere [*Rhie and Romanowicz*, 2004; *Ekström*, 2001]. The seasonality is not pronounced, and begins earlier than expected in mid-March, before the austral winter. Signals extending from 0–360° are large earthquakes, with smaller earthquakes having characteristic 180° patterns for the two opposite great circle paths to the array (e.g., on Dec. 23, Figure 1b). Peak beam power azimuths are concentrated in relatively distinct bands: (1) from about 220–340°, a North Pacific location; (2) across the 120–210° band, likely from the west coast of South America; and (3) a third band centered near 50° azimuth, associated with North Atlantic wave activity.

[1]Scripps Institution of Oceanography, University of California, San Diego, La Jolla, California, USA.

0094-8276/09/2009GL038903$05.00

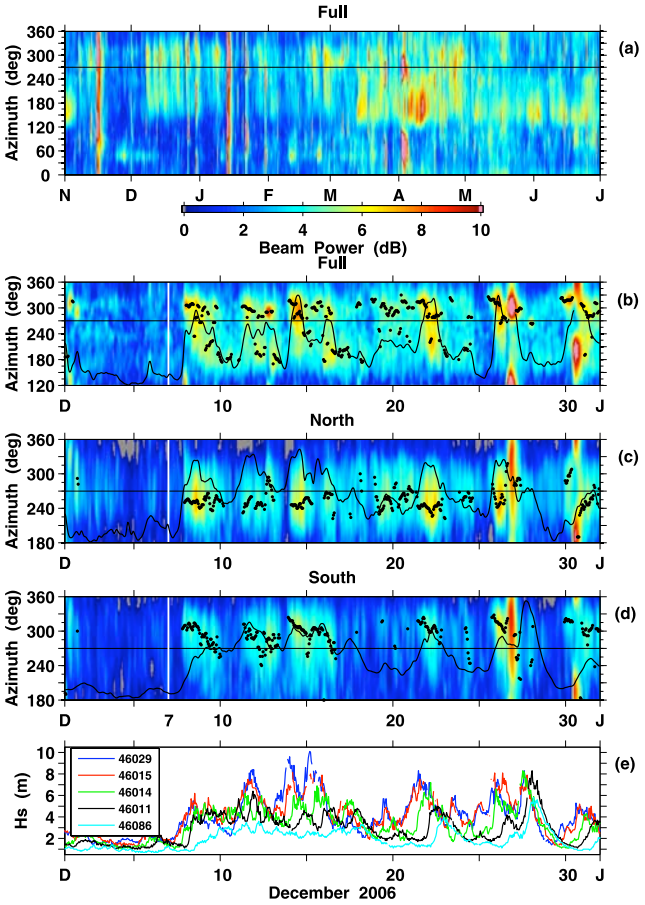

Figure 1. (a) Array beam power with azimuth during Nov. 2006–June 2007. Closer examination of temporal beam power azimuth variability for December 2006 when a series of strong North Pacific storms occurred are shown for the (b) full, (c) north, and (d) south sub-arrays (see Figure 3a), with those times exceeding the 75th percentile threshold (excluding earthquakes) indicated (black dots). Extreme wave heights occurred over the North Pacific deep ocean on Dec. 7 (white lines, see Figure 4a). (e) Wave height at selected NOAA coastal buoys (see Figure 3a) shows the temporal swell variability associated with changes in beam power azimuths. Scaled, lowpass-filtered time series of the 120–360 s hum stack, the mode 1 IG-wave, and the mode 1 buoy Hs are shown in Figures 1b, 1c, and 1d, respectively (black curves).

[6] A series of strong ocean swell events impacted the U.S. West Coast during December 2006 (Figure 1e and Animation S1[1]) [*Tolman*, 2005] (hindcast files available from http://polar.ncep.noaa.gov). Examination of these data in conjunction with hum beam power during this period establishes the "west coast ocean wave-shelf IG wave-hum" relationships during winter. Ocean swell generally propagates along the coast from north-to-south, producing associated high amplitude IG wave episodes. Hourly averages of NOAA 1-min tsunami tide gage data give an estimate of IG wave variability along the west coast (Figure 2), which tracks the beam power and swell variability (Figure 1e) along the coast. Peak IG wave amplitudes are clearly associated with peaks in hum beam power (Figures 1b, 1c, and 1d).

[7] Propagation speed for hum Rayleigh waves (~4 km/s) is much larger than IG wave-generating swell along the coast (~0.014 km/s). This indicates that consistent consecutive north-to-south directional shifts in peak beam power, e.g. observed in the south sub-array (Figure 1d), are likely associated with changes in dominant source locations as the swell propagating from the northwest progressively impacts more southerly coastal locations and is continuously being transformed to IG waves, with certain locations having more favorable characteristics for generating IG waves. The apparent multiple hum source locations along the west coast introduce a high variance in the beam power azimuths, so that dominant source azimuths are best determined from the median peak beam power.

[8] Hum amplitudes depend on IG wave amplitudes and the excitation area [*Webb*, 2008; *Tanimoto*, 2005]. Patterns in beam power suggest that both sub-arrays (see Figure 3a for sub-array configurations) are sensitive to IG waves along the entire coast. The dominant source area for the north sub-array is to the southwest, while for the south sub-array is to the northwest. The median beam power azimuth for the north sub-array (Figure 1c) points to the southwest (251°) and the south sub-array (Figure 1d) points to the northwest (298°). Comparing beam power levels for December 2006 and wave height observations at coastal buoys

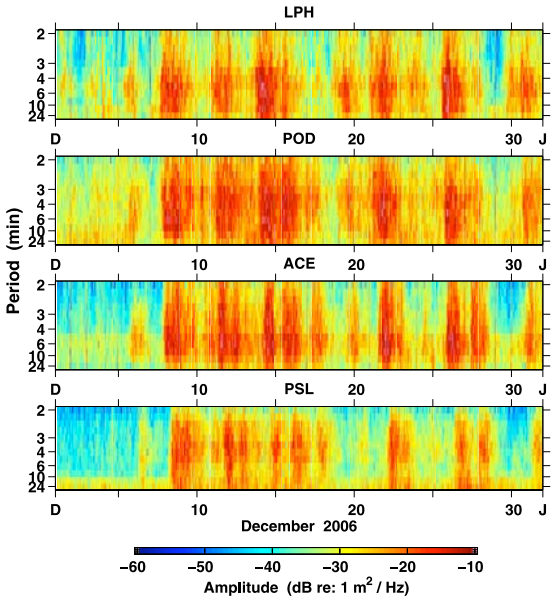

Figure 2. Spectral levels of 1-min tide gauge data in the infragravity-wave band along the U.S. west coast from northern Washington (LPH) to southern California (PSL; see Figure 3a for locations). The typical slight shift in energy to later times results from the lag associated with southward propagation of the IG wave-generating swell along the coast (Figure 1e). No time shift between stations implies IG wave generation from ocean waves at nearly the same time over a long stretch of coastline. The tide gauge data are collected with an acoustic water level sensor having a 3 m dynamic range over 1 s with a 0.1 mm resolution, and averaged to 1 min. The mode 1 principal component of these data is shown in Figure 3b.

[1]Auxiliary materials are available in the HTML. doi:10.1029/2009GL038903.

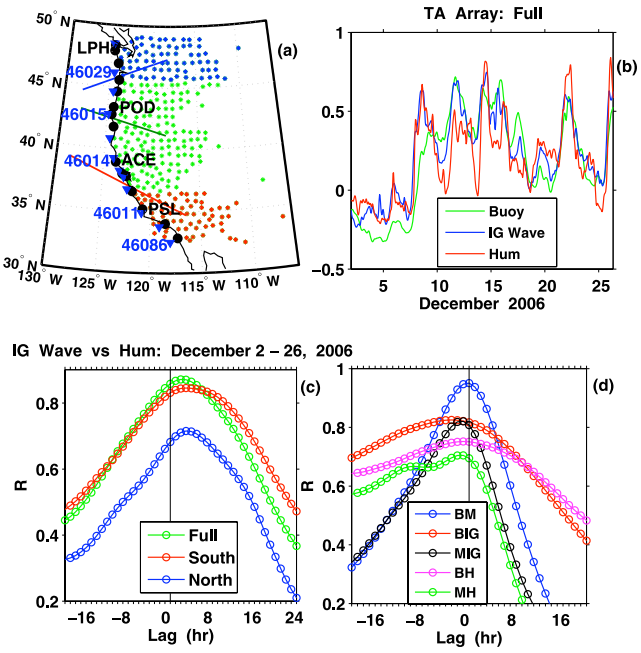

Figure 3. (a) Tide gauge (black circles), buoy (blue triangles), and seismic station (stars) locations. Full TA array analysis includes all 292 stations shown. North (blue) and south (red) sub-arrays consist of 72 and 68 stations, respectively. Great circle vectors associated with the median azimuths associated with the arrays (solid lines). (b) IG wave and buoy Hs mode 1 and hum time series (180–360° azimuth beam power stack) for the full array during December 2006. (c) Lag correlation coefficient (R) functions between the IG wave mode 1 and hum time series (IGH) for the full array and north and south sub-arrays. (d) Lag correlation functions between mode 1 buoy (B), WW3 model (M), and IG wave (IG) times series with the hum stack (H). Negative lags indicate that the first component trails.

(Figure 1e) indicates that high amplitude waves occurring simultaneously along the coast result in stronger hum. Note that peaks in beam power and median azimuths are generally more closely aligned with buoys 46015 and 46014, located nearest the median azimuths for the north sub-array and full array. The full-array median azimuth points north of Cape Mendocino (40.44 N, Figure 3a), consistent with *Rhie and Romanowicz* [2006], where higher wave energy and a wider continental shelf likely contribute to stronger hum generation. Storm track location and orientation relative to the coast also results in a broader coastal region being impacted by swell at the same time, generating IG waves over a larger region nearly simultaneously.

[9] The generally higher beam power amplitudes at the north versus the south sub-array also indicate that the dominant source region is more northerly. In addition, the south sub-array clearly shows the change in back azimuth to the south for individual events, associated with shifting dominant hum generation regions coincident with changing IG wave coastal generation (Figure 2). The change in peak beam power azimuth over these events is consistent with swell propagation time from the initial excitation region along the Pacific Northwest coast to the secondary southern generation region, and may explain lags in hum attributed to IG wave propagation across the North Pacific [*Rhie and Romanowicz*, 2006]. Azimuths near 180° may be associated with IG wave generation along the Baja coast, where wave amplitudes increase after the coastline emerges from Pt. Conception (30.45 N) shadowing effects, which is also suggested by the rapid change in azimuths at the trailing end of strong events for the full TA (Figure 1b).

4. Correlations Between Swell, IG-waves, and Hum

[10] Because ocean swell along coasts generates IG waves that force hum modes, wave data can be used as a proxy for IG wave variability, i.e. higher coastal waves likely force higher hum amplitudes. To establish the underlying correlations between ocean forcing and hum, mode 1 principal component time series were constructed from (1) NOAA 1-min tide gauge data, or significant wave height (Hs) data from either (2) coastal buoys or (3) the WAVEWATCH III [*Tolman*, 2005] ocean swell model. Hum variability was estimated from beam power stacks across azimuth bands for the full array (Figure 1a). IG wave RMS levels over the 400–120 s band (same as TA band) were obtained at 15 stations along the coast (Figure 3a, black circles). Empirical orthogonal function (EOF) analysis of hourly anomalies, with each station's data normalized to unit variance to reduce the impact of site-specific effects on IG wave amplitudes [*Herbers et al.*, 1995b], yields uniform mode 1 EOF variation along the coast. The IG wave mode 1 EOF explains 62% of the variance during the winter (Oct. 2006—Mar. 2007), giving a reasonable estimate of IG wave temporal variability over the shelf.

[11] Peaks in the hum and coastal IG wave mode 1 time series for the full array generally coincide (Figure 3b). The good correlation observed (IGH, Figure 3c) is consistent with hum forcing by IG waves over the shelf, with the IG waves leading the hum by 2 hr at the peak correlation coefficient (R). Lag cross-correlation functions between IG wave mode 1 and the north and south sub-arrays have a lag of 3 hr, consistent with a common hum source. The lags obtained likely result from time-varying source areas along the coast, and reflect the size of the effective hum source region resulting from localized IG wave generation associated with propagating swell. Since the hum originates along the Pacific coast and the 3 hr lag times are much less than the time required for northwesterly swell to propagate across the Oregon-California coast (~16 hr), the hum must be generated along certain dominant coastal regions. Buoy Hs mode 1 was obtained for 12 coastal buoys (Figure 3a, blue triangles) near the tide gauge stations, with corresponding mode 1 determined for WW3 model Hs at grid nodes nearest the buoys. Correlation between wave model and buoy mode 1 is excellent, with the peak R at zero lag (BM, Figure 3d). The IG wave levels correlate well with buoy mode 1 (BIG, Figure 3d), consistent with the link between swell energy and IG wave energy [*Herbers et al.*, 1995a, 1995b]. Interestingly, IG wave mode 1 leads both the buoy and model Hs by a few hours, suggesting that coastal propagation of IG or edge wave energy from the north, where IG-wave generating swell generally first impacts the coast, may provide an important contribution

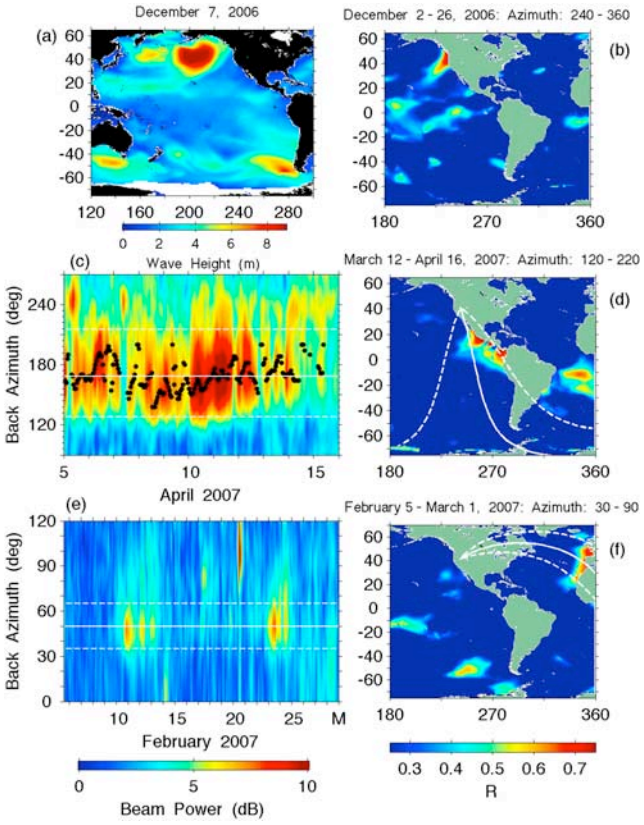

Figure 4. (a) WW3 model wave height on Dec. 7, 2006 00:00 during low hum levels (Figures 1b–1d). (b), (d), and (f) Correlation of hum time series for three azimuth bands with global WW3 wave heights, identifying likely regions of dominant hum generation for periods with low earthquake noise and high hum signals. The median beam power (solid) and extremal bounds (dashed) constrain potential hum source azimuths that are consistent with the correlation maps. (c) and (e) Key hum beam power events during the time period used for the correlations in Figures 4d and 4f, respectively. Titles of Figures 4b, 4d, and 4f indicate the beam power azimuth stack time series that were correlated with wave model Hs.

[*Herbers et al.*, 1995a], and is consistent with the broad peaks for the correlation functions. The correlation between the hum beam power and buoy and model Hs are somewhat lower (BH and MH, Figure 3d), possibly because the hum beam power provides an integrative estimate along parts of the coast not included in the IG mode 1 estimates, and hum energy also arrives at the TA from more distant generation regions.

5. Global Wave Model Correlation with Hum

[12] The relatively good correlation between coastal mode 1 for IG waves and wave model Hs with beam power allows utilization of wave model Hs to identify likely coastal hum source regions. Stacks of beam power for the full TA over the three azimuth bands identified above were correlated with global WW3 model Hs data for time periods when hum signal levels were high and free of earthquake noise. The 240–360° azimuth band stack correlates well only along the coastal region (Figure 4b) identified by the median peak power azimuth estimates (Figure 3a). The extension of the region of high correlation away from the coast results from coherent wave fronts associated with swell propagating from the northwest. This good correlation validates using wave model Hs as a proxy for coastal IG wave variability.

[13] Wave model Hs shows an extreme storm wave event beginning about Dec. 5 and traveling across the North Pacific (Figure 4a and Animation S1). Large storms produce greater amounts of long period wave energy, resulting in higher IG wave levels generated in coastal zones. Beam power levels remain low until waves from this event reach the coast (compare Figures 1b, 1c, 1d, and 4a). This indicates that appreciable hum energy is not excited under very large extreme storms in the deep ocean, and that the Pacific coast of North America is the dominant hum excitation region in the North Pacific.

[14] The highest amplitude hum events observed during the study period occurred during April 2007 (Figure 4c). During April 10–12, an extreme wave event originating from a broad area near 60° S, 140° W (see Animation S1) illuminated a long stretch of the Central American Pacific coast nearly simultaneously. Correlation of the 120–220° azimuth band stack with WW3 model Hs from March 12 to April 16 shows the highest correlation along the Pacific coast of Central America (Figure 4d). Note, that the peak beam power generally shifts to higher back azimuths for individual hum events forced by South Pacific storms (Figure 4c), consistent with hum generation associated with northward propagating swell along the coast. Correlation with model wave height allows differentiation of the Pacific coast source location from other possible South Atlantic regions within the upper bound (225°, dashed lines, Figure 4c).

[15] High amplitude ocean waves regularly impact the coast near the tip of South America, which is a possible source region of IG waves [*Webb et al.*, 1991]. As we have demonstrated that high amplitude waves produce high amplitude hum, hum should be generated there. However, hum time series centered at 150° azimuth (crossing the tip of South America) do not correlate well with wave model Hs. We note that coastlines where the dominant hum signals are detected have components that are nearly orthogonal to the direction to the TA while the tip of South America does not, suggesting that the principal hum propagation direction may depend on coastline orientation and characteristics. The coastal hum excitation mechanism may result in a preferential radiation pattern oriented orthogonal to the coastline. Restricting the analysis band to shorter periods (180–129s, not shown) gives a relatively stronger response from northern source azimuths. Other coastal locations distant from the TA with extreme wave activity are also likely hum excitation regions that may be identifiable with nearer seismometer arrays.

[16] The highest amplitude hum in February originates from the North Atlantic (Figure 4e). Comparison of the wave model Hs (Animation S1) during the two events (February 10 and 23) with beam power shows that the hum increases when the storm waves reach the coast. Correlation of the associated beam time series with wave model Hs show high correlation at the European coast (Figure 4f), consistent with coastal hum generation. Further,

the hum levels were low as large waves passed over the North Atlantic. This shows that little hum energy is excited under extreme storms at deep-ocean North Atlantic locations, in agreement with observations in the North Pacific.

[17] Background hum levels when there are no large waves in the costal regions (e.g., Dec. 4–7, Figures 1b–1d) are potentially generated in the deep ocean by IG waves [*Uchiyama and McWilliams*, 2008; *Webb*, 2008]. However, as moderate-to-lower amplitude waves are ubiquitous along coastlines, IG wave hum forcing on continental shelves must be occurring constantly. Whether low-amplitude hum originates in the deep ocean or only in coastal regions remains uncertain. Regardless, the TA data combined with ocean and IG wave data show that the highest hum levels are generated in particular coastal regions.

6. Conclusions

[18] The demonstrated close inter-relationships of the Earth's hum with coastal infragravity and ocean wave measurements and with wave model simulations show that the dominant hum generation regions are near coasts. Particular Northern Hemisphere coastlines impacted by high ocean waves produce high amplitude hum signals detected by the USArray EarthScope TA. Although high amplitude waves impact coasts in the Southern Hemisphere, hum signals from these regions were not identified with the TA.

[19] **Acknowledgments.** This work was supported by California Department of Boating and Waterways and by U.S. Air Force Research Laboratory, FA8718-07-C-0005.

References

Ekström, G. (2001), Time domain analysis of the Earth's background seismic radiation, *J. Geophys. Res.*, *106*, 26,483–26,494, doi:10.1029/2000JB000086.

Gerstoft, P., and T. Tanimoto (2007), A year of microseisms in southern California, *Geophys. Res. Lett.*, *34*, L20304, doi:10.1029/2007GL031091.

Herbers, T. H. C., S. Elgar, and R. T. Guza (1995a), Generation and propagation of infragravity waves, *J. Geophys. Res.*, *100*, 24,863–24,872, doi:10.1029/95JC02680.

Herbers, T. H. C., S. Elgar, R. T. Guza, and W. C. O'Reilly (1995b), Infragravity-frequency (0.005–0.05 Hz) motions on the shelf. Part II: Free waves, *J. Phys. Oceanogr.*, *25*, 1063–1079, doi:10.1175/1520-0485(1995)025<1063:IFHMOT>2.0.CO;2.

Nishida, K., and N. Kobayashi (1999), Statistical features of Earth's continuous free oscillations, *J. Geophys. Res.*, *104*, 28,741–28,750, doi:10.1029/1999JB900286.

Nishida, K., N. Kobayashi, and Y. Fukao (2000), Resonant oscillations between the solid earth and the atmosphere, *Science*, *287*, 2244–2246, doi:10.1126/science.287.5461.2244.

Rhie, J., and B. Romanowicz (2004), Excitation of Earth's continuous free oscillations by atmosphere-ocean-seafloor coupling, *Nature*, *431*, 552–556, doi:10.1038/nature02942.

Rhie, J., and B. Romanowicz (2006), A study of the relation between ocean storms and the Earth's hum, *Geochem. Geophys. Geosyst.*, *7*, Q10004, doi:10.1029/2006GC001274.

Suda, N., K. Kazunari, and Y. Fukao (1998), Earth's background free oscillations, *Science*, *279*, 2089–2091, doi:10.1126/science.279.5359.2089.

Tanimoto, T. (2005), The oceanic excitation hypothesis for the continuous oscillations of the Earth, *Geophys. J. Int.*, *160*, 276–288, doi:10.1111/j.1363-246X.2004.02484.x.

Tolman, H. L. (2005), Manual and wave user system documentation of WAVEWATCH-III version 2.22, U.S. Dep. of Comm., Washington, D. C.

Uchiyama, Y., and J. C. McWilliams (2008), Infragravity waves in the deep ocean: Generation, propagation, and seismic hum excitation, *J. Geophys. Res.*, *113*, C07029, doi:10.1029/2007JC004562.

Webb, S. C. (2007), The Earth's "hum" is driven by ocean waves over the continental shelves, *Nature*, *445*, 754–756, doi:10.1038/nature05536.

Webb, S. C. (2008), The Earth's hum: The excitation of Earth's normal modes by ocean waves, *Geophys. J. Int.*, *174*, 542–566, doi:10.1111/j.1363-246X.

Webb, S. C., X. Zhang, and W. Crawford (1991), Infragravity waves in the deep ocean, *J. Geophys. Res.*, *96*, 2723–2736, doi:10.1029/90JC02212.

P. D. Bromirski and P. Gerstoft, Scripps Institution of Oceanography, University of California, San Diego, La Jolla, CA, USA. (pbromirski@ucsd.edu)